Plaque Neovascularization Is Increased in Ruptured Atherosclerotic Lesions of Human Aorta

Implications for Plaque Vulnerability

Pedro R. Moreno, MD; K. Raman Purushothaman, MD; Valentin Fuster, MD, PhD; Dario Echeverri, MD; Helena Truszczynska, PhD; Samin K. Sharma, MD; Juan J. Badimon, PhD; William N. O'Connor, MD

Background—Growth of atherosclerotic plaques is accompanied by neovascularization from vasa vasorum microvessels extending through the tunica media into the base of the plaque and by lumen-derived microvessels through the fibrous cap. Microvessels are associated with plaque hemorrhage and may play a role in plaque rupture. Accordingly, we tested this hypothesis by investigating whether microvessels in the tunica media, the base of the plaque, and the fibrous cap are increased in ruptured atherosclerotic plaques in human aorta.

Methods and Results—Microvessels, defined as CD34-positive tubuloluminal capillaries recognized in cross-sectional and longitudinal profiles, were quantified in 269 advanced human plaques by bicolor immunohistochemistry. Macrophages/T lymphocytes and smooth muscle cells were defined as CD68/CD3-positive and α-actin–positive cells. Total microvessel density was increased in ruptured plaques when compared with nonruptured plaques ($P=0.0001$). Furthermore, microvessel density was increased in lesions with severe macrophage infiltration at the fibrous cap ($P=0.0001$) and at the shoulders of the plaque ($P=0.0001$). In addition, microvessel density was also increased in lesions with intraplaque hemorrhage ($P=0.04$) and in thin-cap fibroatheromas ($P=0.038$). Logistic regression analysis identified plaque base microvessel density ($P=0.003$) as an independent correlate to plaque rupture.

Conclusions—Thus, neovascularization as manifested by the localized appearance of microvessels is increased in ruptured plaques in the human aorta. Furthermore, microvessel density is increased in lesions with inflammation, with intraplaque hemorrhage, and in thin-cap fibroatheromas. Microvessels at the base of the plaque are independently correlated with plaque rupture, suggesting a contributory role for neovascularization in the process of plaque rupture. **(*Circulation*. 2004;110:2032-2038.)**

Key Words: atherosclerosis ■ plaque ■ inflammation ■ aorta

Nourishment of normal blood vessels is accomplished by oxygen diffusion from the lumen of the vessel or from adventitial vasa vasorum.[1] When vessel wall thickness exceeds the effective diffusion distance of oxygen, vasa vasorum proliferate in the inner layers of the vessel wall, where they are normally absent. Vasa vasorum are present in most arteries, including the aorta and coronary, carotid, and femoral arteries.[1] Pathological neovascularization of the vessel wall is a consistent feature of atherosclerotic plaque development and progression of the disease.[2,3] Furthermore, microvessels play a role in plaque hemorrhage associated with the development of symptoms in cerebrovascular disease.[4,5] In addition, microvessels are increased in coronary lesions from patients with acute myocardial infarction, suggesting a potential role for microvessels in plaque rupture.[6,7]

Histological features associated with plaque rupture include a large lipid core, thin fibrous cap, and increased inflammation.[8] Furthermore, rupture of the internal elastic lamina (IEL) is also seen in complex plaques.[9] Recently, microvessel-related intraplaque hemorrhage has been associated with lipid-core expansion through the accumulation of free cholesterol from erythrocyte membranes.[10] In addition, intraplaque hemorrhage is a potent stimulus for macrophage activation and foam cell formation, thereby increasing plaque inflammation.[11] Therefore, microvessels may play a role in plaque rupture.

The present study was designed to test the hypothesis that microvessel density is increased in atherosclerotic lesions with plaque rupture and to investigate independent histological features associated with plaque rupture.

Methods

Full-thickness aortic wall histological sections from 269 lesions were taken sequentially at autopsy from 24 male patients (mean±SD age,

Received June 26, 2002; de novo received March 18, 2004; revision received June 22, 2004; accepted June 22, 2004.

From the Cardiovascular Institute (P.R.M., K.R.P., V.F., S.K.S., J.J.B.), Mount Sinai School of Medicine, New York, NY, and the Linda and Jack Gill Heart Institute (P.R.M., D.E., H.T., W.N.O.), University of Kentucky, Lexington.

Correspondence to Pedro R. Moreno, MD, Cardiovascular Institute, One Gustave L. Levy Place, Box 1030, New York, NY 10029. E-mail pedro.moreno@msnyuhealth.org

Circulation **is available at http://www.circulationaha.org** **DOI: 10.1161/01.CIR.0000143233.87854.23**

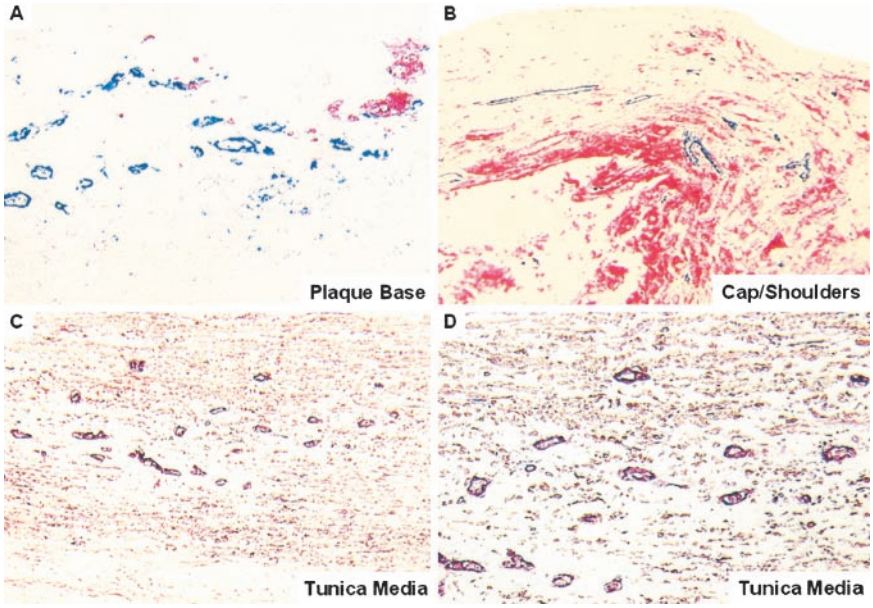

Figure 1. A, High-power image of microvessels at plaque base, detected with monoclonal endothelial cell marker CD34 linked to blue chromogen, admixed with few CD68/CD3-positive inflammatory cells linked to red chromogen. B, High-power image (×40) from cap and shoulder region of lipid-rich plaque, showing CD34-positive microvessels in blue contrasting sharply with CD68/CD3-positive inflammatory cells linked to red chromogen. C, Medium-power image (×20) of microvessels at tunica media from lipid-rich plaque, demonstrated with monoclonal endothelial cell marker CD34 linked to purple chromogen contrasting with smooth muscle cells of media in brown chromogen stained with α-actin. D, High-power image (×40) of media from same area as in C, showing CD34-positive microvessels in purple chromogen contrasting with smooth muscle cells surrounding neovessels in brown chromogen stained with α-actin.

61±16 years; range, 29 to 89 years). The aorta was slit open longitudinally, and the intima was washed with saline and then examined visually. On gross examination, aortas had diffuse atherosclerotic lesions with variably distanced spaces between plaques. No aneurysms were observed. A 20-cm aortic segment from the lower thoracic aorta extending into the abdominal aorta above the renal arteries was selected. Individual atherosclerotic plaques raised above the surface with a long axis >0.75 cm were studied.[12] A 1.0-cm long by 0.5-cm wide sample with an edge of normal tissue was obtained for each plaque. The minimum distance between plaques was 0.5 cm. A total of 12 serial sections from each specimen were cut and stained by (1) hematoxylin and eosin (n=3); (2) elastic trichrome method (n=3); (3) double-labeled immunochemicals for endothelial cells and inflammatory cells (macrophages/T lymphocytes) with CD34 and CD68/CD3, respectively (n=3); and (4) double-labeled immunochemicals for endothelial cells and smooth muscle cells with CD34 and α-actin, respectively (n=3). The average value (total numbers divided by 3) is reported for each stain.

Immunohistochemistry

Labeling was performed on formalin-fixed, paraffin-embedded, 4-μm tissue sections on polylysine-coated–plus glass slides. Tissue sections were deparaffinized and then pretreated with sodium citrate–antigen retrieval at 5-minute intervals up to a total of 15 minutes. After endogenous peroxidase activity was blocked with 10% H_2O_2 in methanol, sections were subjected to double labeling. Primary monoclonal mouse anti-human antibodies of the IgG1 class (DAKO Corp) included the CD34 endothelial clone Qbend-10 at 1:30 dilution, CD68 macrophage clone KP-1 at 1:100 dilution/CD3 T-lymphocyte clone at 1:50 dilution, and α-actin smooth muscle clone at 1:50 dilution. Affinity-purified, secondary anti-mouse IgG antibodies with Western blot–confirmed specificity were obtained from Vector Diagnostics in an avidin-biotin–conjugated Elite kit PK6102. Double immunohistochemistry was systematically performed in all sections by applying 2 entirely separate sets of contrasting bicolor preparations to each block. The first paired bicolor preparation used a blue (alkaline phosphatase SK 5300, Vector) and red (alkaline phosphatase SK 5100, Vector) chromogen reaction to distinguish endothelial microvessel cells from inflammatory cells (macrophage/lymphocyte cocktail), respectively, as shown in Figure 1A and 1B. The second paired bicolor preparation used a purple (peroxidase VIP SK 4600, Vector) and brown (diaminobenzidine tetrachloride, Sigma) chromogen reaction to distinguish endothelial microvessel cells (CD34) from smooth muscle cells (α-smooth muscle actin), respectively, as shown in Figure 1C and 1D. Specificity of all antibodies was confirmed by routine positive and negative controls for each stain in human tonsil and bowel tissue to exclude nonspecific binding of the primary antibody.

Morphometry

Neovascularization

Microvessels were defined as tubuloluminal CD34-positive capillaries recognized in cross-sectional and longitudinal profiles as identified by double immunohistochemistry with CD34/CD68-CD3 in the intima and CD34/smooth muscle actin in the tunica media with a ×40 magnification objective. Microvessel density was calculated by taking the total number of microvessels and dividing by plaque area (mm^2). Quantification was regionally tabulated for 3 contiguous, nonoverlapping transmural sites for each individual section, including (1) microvessels located within the tunica media, (2) microvessels located at the base of the plaque, and (3) microvessels located at the fibrous cap and shoulders. Because we encountered a highly variable quantity of adventitial tissue in these sections, we opted to exclude adventitial measurements from the analysis. Finally, total microvessel density (sites 1, 2, and 3 combined divided by plaque area) is also reported.

Macrophages and T Lymphocytes

Inflammatory cells were defined as CD68/CD3-positive mononuclear round cells per high-power field with the ×40 magnification objective. Inflammation was tabulated for 2 different regions of the atherosclerotic lesion including the fibrous cap and plaque shoulders. Severity of inflammation was scored as 0 (≤5 cells), 1 (6 to 25 cells), and 2 (≥25 cells).

Rupture of the IEL and other measurements, including minimum fibrous cap thickness, total plaque area, and lipid-core area, were quantified by nonautomated ocular micrometry and computerized planimetry, as previously reported.[13] Data reported in this study are from a new set of aortas not included in our previous publication.[13]

Histological Classification

Lesions with fibrous-cap rupture were defined as plaques with discontinuation of the fibrous cap associated with hemorrhage or thrombus, as shown in Figure 2A. Lesions without fibrous cap rupture were defined by using a modified version of the American Heart Association classification[14] as fibrocalcific (class Vb and Vc) and lipid-rich (class IV and Va) plaques. Fibrocalcific plaques are usually devoid of a lipid core. Therefore, no fibrous cap could be consistently identified. Therefore, for neovessel comparisons with

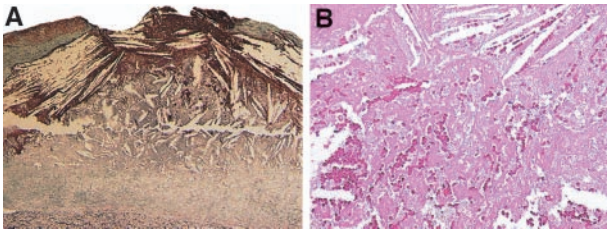

Figure 2. A, Histological example of fibrous cap rupture, showing discontinuation of fibrous cap in lipid-rich plaque (elastica trichrome stain). Magnification ×10. B, High-power view of human aortic plaque with intra plaque hemorrhage, showing red blood cell extravasation within lipid core (hematoxylin and eosin stain). Magnification ×40.

lipid-rich and ruptured plaques in the fibrous cap/shoulder category, the corresponding luminal part of fibrocalcific plaques was evaluated and included in the analysis.

Lesions With Plaque Hemorrhage

Hemorrhage was defined as red blood cell extravasation within the plaque, as shown in Figure 2B. Serial sectioning was performed in every case of plaque hemorrhage to exclude fibrous cap rupture as the cause of hemorrhage. With these criteria, plaque hemorrhage was observed only in lipid-rich plaques.

Lesions With Thin, Fibrous Cap

Fibrous cap thickness ≤60 μm was defined as thin-cap fibroatheromas, as previously reported,[15] and was observed only in lipid-rich plaques.

Lesions With Inflammation

Mild (score 0) inflammation was compared with moderate (score 1) and severe (score 2) inflammation within the fibrous cap and shoulder regions of the plaque, as described earlier.

Statistical Analysis

Data are presented as mean±SEM. For 2-group comparisons, gaussian-distribution samples were compared by the 2-tailed Student *t* test, preceded by Levene F test for equality of variances. Nongaussian-distribution samples were compared by the Mann-Whitney nonparametric test. For multiple comparisons, 1-way ANOVA was used. Discrete variables were compared with the χ^2 test. The following variables were used in the analysis: plaque rupture and cap thickness ≤60 μm (dichotomous variables); cap inflammation and shoulder inflammation score (ordinal variables with values of 0, 1, or 2); media neovessel density; plaque-base neovessel density; cap/shoulder neovessel density; total neovessel density; plaque area; and lipid area (continuous variables). Plaque rupture was the outcome variable. To identify independent correlates with plaque rupture, univariate analysis consisting of cross tabulations of each variable by plaque rupture was performed. Continuous variables were categorized on the basis of quartiles for cross tabulation. Bivariate correlation coefficients between variables were also computed to identify colinearity. When the correlation coefficient between 2 variables was >0.6, only 1 was selected in the final model. The selection was based on the results of the univariate analysis and taking into account the significance level. Variables exhibiting statistical significance in the univariate logistic regression were chosen and then used in a multiple logistic regression model. SPSS 12.0 software was used for the analysis. Probability values <0.05 were considered significant.

Results

Lesions With Fibrous-Cap Rupture

Neovessel density in ruptured and nonruptured plaques is shown in Figure 3. Total neovessel density was increased in

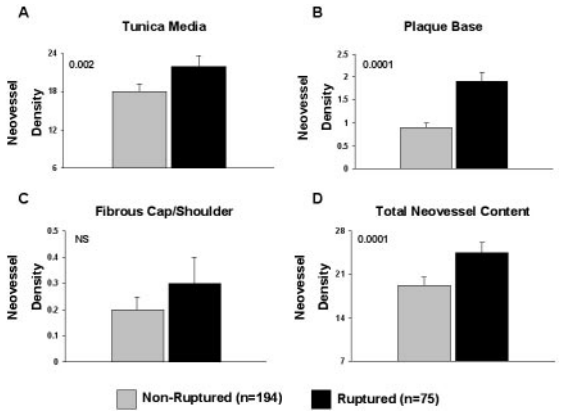

Figure 3. Composite graph displaying mean and SEM of neovessel density within plaque and tunica media in ruptured and nonruptured plaques. A, Higher neovessel density in ruptured plaques in tunica media; B, higher neovessel density in ruptured plaques at base of the plaque; C, similar neovessel density at fibrous cap and shoulder areas; D, higher total neovessel density in ruptured plaques when compared with nonruptured plaques.

ruptured plaques when compared with nonruptured plaques (P=0.0001). Segmental analysis showed increased neovessel density at the tunica media (P=0.002) and at the base of the plaque (P=0.001) and a similar density in fibrous cap/shoulders (P=NS).

Lesions Without Fibrous-Cap Rupture

Neovessel densities in fibrocalcific and lipid-rich plaques were compared with those of ruptured plaques, as shown in Figure 4. Total neovessel density was lower in fibrocalcific plaques when compared with lipid-rich and ruptured plaques (P=0.0001). Segmental analysis showed decreased neovessel density in fibrocalcific plaques when compared with lipid-rich and ruptured plaques in all areas studied (P=0.0001). Neovessel density in the tunica media and at the fibrous cap was similar between lipid-rich and ruptured plaques (P=NS).

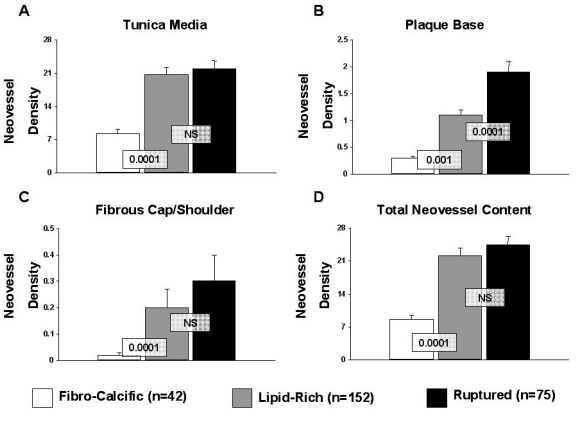

Figure 4. Composite graph displaying mean and SEM of neovessel density within plaque and tunica media in fibrocalcific, lipid-rich, and ruptured plaques. Neovessel were scant in fibrocalcific but abundant in lipid-rich and ruptured plaques. A, Neovessel density in tunica media; B, neovessel density at base of plaque; C, neovessel density at fibrous cap and shoulder areas; D, total neovessel density.

TABLE 1. Neovessel Density in Lipid-Rich Plaques With Hemorrhage and Thin, Fibrous Cap

Neovessel Location	Hemorrhage (n=44)	No Hemorrhage (n=108)	P	Thin Cap (n=34)	No Thin Cap (n=118)	P
Tunica media density	26±4.15	19±1.35	0.058	30±5.59	18±1.07	0.037
Plaque base density	2.1±0.41	0.8±0.05	0.004	1.8±0.46	1.0±0.10	0.08
Cap-shoulder density	0.5±0.16	0.2±0.08	0.036	0.3±0.08	0.3±0.13	0.99
Total neovessel density	29±4.7	20±1.5	0.042	32±6.1	19±1.3	0.038

However, at the base of the plaque, neovessel density was higher in ruptured plaques when compared with lipid-rich plaques ($P=0.0001$).

Lesions With Plaque Hemorrhage

Plaque hemorrhage without fibrous-cap rupture was seen only in lipid-rich lesions. Therefore, comparisons were performed within this category only (Table 1). Plaque base, cap/shoulder, and total neovessel densities were higher in lipid-rich lesions with hemorrhage when compared with lipid-rich lesions without hemorrhage ($P<0.05$). A tendency toward higher neovessel density in the tunica media was also observed ($P=0.058$).

Lesions With Thin, Fibrous Cap

Intact thin fibrous caps were present only in lipid-rich lesions. Therefore, comparisons were performed within this category only (Table 1). Total neovessel density was higher in thin-cap when compared with non–thin cap lesions ($P=0.038$; Table 1).

Lesions With Inflammation

Total neovessel density was lowest in lesions with mild inflammation, moderate in lesions with moderate inflammation, and highest in lesions with severe inflammation, as quantified at the fibrous cap and plaque shoulders ($P=0.0001$; Table 2). Finally, rupture of the IEL, lipid area, and inflammatory scores were higher and cap thicknesses lower in ruptured plaques when compared with lipid-rich and fibrocalcific plaques ($P=0.0001$; Table 3).

Correlates of Plaque Rupture

Univariate analysis identified significant variables as shown in Table 4. Furthermore, bivariate correlations identified colinearity in 5 pairs of variables, as follows: (1) Media neovessel density was correlated with total neovessel density ($r=0.996$); (2) plaque-base neovessel density was correlated with total neovessel density ($r=0.711$); (3) plaque-base neovessel density was correlated with media neovessel density ($r=0.659$); (4) lipid area was correlated with plaque area ($r=0.853$); and (5) cap inflammation was correlated with shoulder inflammation ($r=0.644$).

Of these 5 pairs of variables, plaque base neovessel density, lipid area, and cap inflammation exhibited more powerful statistical correlation with plaque rupture when compared with their colinear variables in the univariate analysis (as shown in Table 4) and were included in the final model, along with cap thickness ≤ 60 μm and rupture of the IEL. The final model had a good fit, as indicated by the Nagelkerke r^2 value of 0.69, a sensitivity of 94%, a specificity of 85%, and 92% overall correct prediction. All correlates included in the final model were statistically significant as shown in Table 4: A cap thickness ≤ 60 μm resulted in a significantly higher probability of plaque rupture than did cap thickness >60 μm (odds ratio, 23.4; $P<0.001$); rupture of the IEL resulted in a significantly higher probability of plaque rupture than nonrupture of the IEL (odds ratio, 13.7; $P<0.001$); a higher cap inflammation score increased the odds of plaque rupture >3-fold (odds ratio, 3.12; $P=0.002$), as did high microvessel density at the base of the plaque (odds ratio, 1.47; $P=0.003$) and large lipid area (odds ratio, 1.15; $P=0.037$).

Discussion

In this study of atherosclerotic neovascularization, we compared microvessel density in ruptured and nonruptured human plaques. Systematic quantification by computerized planimetry and ocular micrometry in bicolor contrasting immunostained sections documented increased microvessel density in ruptured plaques. Microvessel density was also increased in lipid-rich and ruptured plaques when compared with fibrocalcific lesions. Furthermore, lesions with intraplaque hemorrhage and a thin, fibrous cap also

TABLE 2. Neovessel Density in Advanced Lesions Evaluated by the Degree of Plaque Inflammation

	Fibrous Cap				Plaque Shoulder			
Neovessel Location	Mild (n=74)	Moderate (n=119)	Severe (n=76)	P	Mild (n=47)	Moderate (n=81)	Severe (n=141)	P
Tunica media density	12.9±1.3	20.9±1.9	22.6±1.6	0.001	9.7±1.05	19.6±2.2	22.1±1.4	0.0001
Plaque base density	0.66±0.08	1.3±0.16	1.8±0.22	0.0001	0.49±0.13	1.05±0.12	1.6±0.17	0.0001
Cap-shoulder density	0.11±0.05	0.30±0.1	0.34±0.1	0.22	0.01±0.01	0.26±0.11	0.35±0.08	0.61
Total neovessel density	13.7±1.4	23.9±2.2	24.7±1.9	0.0001	10.2±1.2	20.9±2.4	24.1±1.7	0.0001

Mild indicates <5 cells per high-power field (HPF); moderate, 6 to 25 cells per HPF; and severe, >25 cells per HPF.

TABLE 3. Histological Characteristics of Fibrocalcific, Lipid-Rich, and Ruptured Plaques

Classification	No. (%)	Plaque Area, mm^2	Lipid Area, mm^2	Cap Thickness, μm	Ruptured IEL, No. (%)	Inflammation Score	
						Fibrous Cap	Shoulder
Fibrocalcific plaques	42 (16)	10.4±0.88	2.4±0.38	...	26 (62)	0.1±0.07	0.3±0.08
Lipid-rich plaques	152 (66)	9.4±0.48	3.5±0.28	28±20	95 (63)	1.0±0.06	1.5±0.05
Ruptured plaques	75 (28)	12.7±0.77	6.2±0.44	33±2.0	68 (91)	1.5±0.06	1.7±0.06
Total and *P* value	269 (100)	0.0001	0.0001	0.0001	0.0001	0.0001	0.0001

Abbreviations are as defined in text.

displayed higher microvessel density. In addition, microvessel density was low in lesions with mild inflammation and increasingly higher in lesions with moderate and severe inflammation. Finally, multiple regression analysis identified microvessels at the base of the plaque as an independent correlate of plaque rupture, along with established variables including a thin cap, inflammation, lipid area, and rupture of the IEL.

Our understanding of the role of neovascularization in atherosclerotic plaques is evolving and may include several processes. As part of the cellular inflammatory response to injury, microvessels contribute to the phase of repair. Once phagocytosis has removed the injurious agent, nonleukocytic mesenchymal elements such as neovascularization play an important role in repair.[16] In pathological conditions, neovascularization varies from a transient contribution to healing (wound granulation tissue that regresses) to a permanent contribution for tissue regeneration. If the injurious agent persists, various patterns of chronic inflammation can develop. Newly formed microvessels coexists with osteoclast-like foreign-body giant cells (engulfing cholesterol crystals), necrosis, immune cells, and macrophages localizing an expanding granulomatous-like reaction, which characterizes complex atherosclerosis within the arterial wall.[17] Recently, inhibition of angiogenesis by endostatin reduced plaque growth by 70% to 85%, suggesting a role for microvessels in progression of the disease.[18]

The origin of atherosclerotic neovascularization was elucidated by Kumamoto et al,[19] who established communication with adventitial vasa vasorum in 97% of human coronary plaque microvasculature. The relation between microvessels, inflammation, and lipid-core expansion in advanced atherosclerosis is also evolving. Microvessels facilitate blood-derived inflammatory cells to penetrate through the vessel wall, increasing macrophage infiltration. Furthermore, inflammation also increases microangiogenic activity, amplifying macrophage recruitment.[20] This study identified an incremental relation between neovascularization and inflammation, supporting a synergistic association in advanced disease. However, the association between neovascularization and plaque rupture

TABLE 4. Univariate and Mutivariate Analysis to Identify Correlates of Plaque Rupture

	P	Odds Ratio	95% Confidence Intervals	
			Lower	Upper
Univariate analysis				
Media neovessel density	0.087	1.01	0.99	1.028
Plaque base neovessel density	<0.001	1.42	1.17	1.72
Cap/shoulder neovessel density	0.27	1.17	0.89	1.5
Total neovessel density	0.048	1.01	1	1.03
Rupture of IEL	<0.001	5.86	2.55	13.44
Plaque area	<0.001	1.09	1.05	1.15
Lipid area	<0.001	1.29	1.18	1.41
Cap thickness <60 μm	<0.001	36.92	16.55	82.36
Cap inflammation score	<0.001	4.82	3.02	7.69
Shoulder inflammation score	<0.001	2.91	1.83	4.62
Multivariate analysis				
Cap thickness <60 μm	<0.001	23.5	9.3	58.9
Rupture of IEL	<0.001	13.7	4.02	46.9
Cap inflammation score	0.002	3.12	1.51	6.45
Plaque base neovessel density	0.003	1.47	1.14	1.9
Lipid area	0.037	1.15	1.01	1.32

Abbreviations are as defined in text.

may be mechanistically or casually related. Microvessels are traditionally increased in large plaques. Therefore, increased microvessel density in ruptured plaques may be a reflection of plaque size. Nevertheless, microvessel density was independently associated with plaque rupture. Furthermore, large, fibrocalcific plaques exhibited the lowest microvessel density. In addition, recent studies suggest that microvessel leakage may contribute to lipid-core expansion preceding plaque rupture.[21] As a result, some evidence for a mechanistic association is emerging. With the advent of potent imaging technology (magnetic resonance imaging or ultrasound-directed microbubble imaging), neovascularization may constitute a suitable target to completely elucidate this issue.[22,23]

Previous reports have studied plaque neovascularization in advanced atherosclerosis in carotid endarterectomy specimens.[24,25] However, these studies did not evaluate neovascularization across the vessel wall. Our study in aortic sections identified neovessel density within the plaque to be lower than that within the tunica media. Nevertheless, only neovessels at the base of the plaque were independently associated with plaque rupture. Furthermore, correlations between macrophage infiltration in high-risk zones, lipid area and minimum cap thickness (in microns), are also needed to address independent relations between microvessel density and plaque rupture. Thus, our results expand knowledge in providing a careful evaluation of neovessel density across the vessel wall, with a segmental correlation between microvessel density and plaque rupture, independent of traditional features of vulnerability.

Finally, the low microvessel density in fibrocalcific plaques requires further investigation. These lesions exhibited a large plaque area with a very minimal amount of lipid. This observation may be important in the understanding of plaque stabilization, but more studies are needed to elucidate this issue.[26]

Study Limitations

The abdominal aorta may be considered avascular tissue. Nevertheless, previous studies have shown vasa supplying the abdominal aorta arising from the origin of lumbar and mesenteric arteries.[27] Data are reported as the number of neovessels per plaque area. Medial area may have been included when reporting medial neovessel density. Nevertheless, data were collected for plaque area only and may limit the interpretation of the results. In addition, coronary lesions were not investigated in this study. Previous extensive experience in aortic disease influenced our decision to use aortic instead of coronary plaques. As a result, the interpretation of results should be maintained in the setting of aortic disease. Finally, despite the fact that CD34 immunostaining is specific for endothelial cells in proliferating vessels, it cannot differentiate between microcapillaries and microlymphatics. Lymphangiogenesis from large-vessel origin (thoracic duct) may be identified with specific markers.[28,29] Therefore, differentiation between microvessels and microlymphatics requires further investigation.

Conclusion

Vessel-wall and plaque microvessels are increased in ruptured atherosclerotic plaques, suggesting a link between microvessels and plaque instability. Future prospective studies evaluating plaque microvessels in vivo are needed to completely elucidate this issue.

Acknowledgments

The authors are indebted to Terry Lacy and Robin King for their technical assistance and to Drs Frederick C. DeBeer, Jay W. Mason, James E. Muller, and David C. Booth for their invaluable support.

References

1. Heistad D, Marcus ML. Role of vasa vasorum in nourishment of the aorta. *Blood Vessels*. 1979;16:225–238.
2. Jeziorska M, Woolley DE. Neovascularization in early atherosclerotic lesions of human carotid arteries: its potential contribution to plaque development. *Hum Pathol*. 1999;30:919–925.
3. Barger AC, Beeuwkes R, Lainey L, et al. Hypothesis: vasa vasorum and neovascularization of human coronary arteries. *N Engl J Med*. 1984;310:175–177.
4. Milei J, Parodi JC, Fernandez G, et al. Carotid rupture and intraplaque hemorrhage: immunophenotype and role of cells involved. *Am Heart J*. 1998;136:1096–1105.
5. Mofidi R, Crotty TB, McCarthy P, et al. Association between plaque instability, angiogenesis and symptomatic carotid occlusive disease. *Br J Surg*. 2001;88:945–950.
6. Barger AC, Beeuwkes R. Rupture of coronary vasa vasorum as a trigger of acute myocardial infarction. *Am J Cardiol*. 1990;66: 41G–43G.
7. Tenaglia AN, Peters KG, Sketch MH Jr, et al. Neovascularization in atherectomy specimens from patients with unstable angina: implications for pathogenesis of unstable angina. *Am Heart J*. 1998;135: 10–14.
8. Falk E, Shah PK, Fuster V. Coronary plaque disruption. *Circulation*. 1995;92:657–671.
9. Davies M. Stability and instability: two faces of coronary atherosclerosis: the Paul Dudley White Lecture, 1995. *Circulation*. 1996;94: 2013–2020.
10. Kolodgie FD, Gold HK, Burke AP, et al. Intraplaque hemorrhage and progression of coronary atheroma. *N Engl J Med*. 2003;349:2316–25.
11. Kockx MM, Cromheeke KM, Knaapen MW, et al. Phagocytosis and macrophage activation associated with hemorrhagic microvessels in human atherosclerosis. *Arterioscler Thromb Vasc Biol*. 2003;23: 440–446.
12. Davies MJ, Richardson PD, Woolf N, et al. Risk of thrombosis in human atherosclerotic plaques: role of extracellular lipid, macrophage, and smooth muscle cell content. *Br Heart J*. 1993;69:377–381.
13. Moreno PR, Purushothaman KR, Fuster V, et al. Intimomedial interface damage and adventitial inflammation is increased beneath disrupted atherosclerosis in the aorta: implications for plaque vulnerability. *Circulation*. 2002;105:2502–2509.
14. Stary HC, Chandler AB, Dinsmore RE, et al. A definition of advanced types of atherosclerotic lesions and a histological classification of atherosclerosis: a report from the Committee on Vascular Lesions of the Council on Arteriosclerosis, American Heart Association. *Circulation*. 1995;92:1355–1374.
15. Moreno PR, Lodder RA, Purushothaman KR, et al. Detection of lipid pool, thin fibrous cap, and inflammatory cells in human aortic atherosclerotic plaques by near-infrared spectroscopy. *Circulation*. 2002; 105:923–927.
16. General pathology: acute and chronic inflammation. In: Cotran RS, Kumar V, Collins T, eds. *Robbins Pathologic Basis of Disease*, 6th ed. Philadelphia, Pa: WB Saunders Co; 1999:79–83.
17. Raines EW, Rosenfeld ME, Ross R. The role of macrophages. In: Fuster V, Ross R, Topol E, eds. *Atherosclerosis and Coronary Artery Disease*. Philadelphia, Pa: Lippincott-Raven Publishers; 1996: 539–555.
18. Moulton KS, Heller E, Konerding MA, et al. Angiogenesis inhibitors endostatin or TNP-470 reduce intimal neovascularization and plaque

growth in apolipoprotein E–deficient mice. *Circulation*. 1999;99:1726–1732.
19. Kumamoto M, Nakashima Y, Sueishi K. Intimal neovascularization in human coronary atherosclerosis. *Hum Pathol*. 1995;26:450–456.
20. Polverini PJ, Cotran RS, Gimbrone MA Jr, et al. Activated macrophages induce vascular proliferation. *Nature*. 1977;269:804–806.
21. Arbustini E, Morbini P, D'Armini AM, et al. Plaque composition in plexogenic thromboembolic pulmonary hypertension: the critical role of thrombotic material in pultaceous core formation. *Heart*. 2002;88:177–182.
22. Leong-Poi H, Christiansen J, Klibanov AL, et al. Noninvasive assessment of angiogenesis by ultrasound and microbubbles targeted to α_v integrins. *Circulation*. 2003;107:455–460.
23. Casscells W, Hassan K, Vaseghi MF, et al. Plaque blush, branch location, and calcification are angiographic predictors of progression of mild to moderate coronary stenoses. *Am Heart J*. 2003;145:813–820.
24. McCarthy MJ, Loftus IM, Thompson MM, et al. Angiogenesis and the atherosclerotic carotid plaque: an association between symptomatology and plaque morphology. *J Vasc Surg*. 1999;30:261–268.
25. de Boer OJ, van der Wal AC, Teeling P, et al. Leucocyte recruitment in rupture prone regions of lipid-rich plaques: a prominent role for neovascularization? *Cardiovasc Res*. 1999;41:443–449.
26. Corti R, Fuster V, Fayad ZA, et al. Lipid lowering by simvastatin induces regression of human atherosclerotic lesions: two years' follow-up by high-resolution noninvasive magnetic resonance imaging. *Circulation*. 2002;106:2884–2887.
27. Williams JK, Heistad DD. Structure and function of vasa vasorum. *Trends Cardiovasc Med*. 1996;6:53–57.
28. Breiteneder-Geleff S, Soleiman A, Kowalski H, et al. Angiosarcomas express mixed endothelial phenotypes of blood and lymphatic capillaries: podoplanin as a specific marker for lymphatic endothelium. *Am J Pathol*. 1999;154:385–394.
29. Wigle JT, Oliver G. Prox1 function is required for the development of the murine lymphatic system. *Cell*. 1999;98:769–778.